

Study of the Dye Sensitized Solar Cells I–V characterisation process

Ala Eddinne Touihri¹, Tarek Azizi, Rached Gharbi²

Université de Tunis, ENSIT, LSDE C3S, 1008 Montfleury, Tunisia.

¹alaeddinnet@gmail.com

²rached.gharbi@esst.rnu.tn

Abstract—In this work we present an experimental investigation of the Dye Sensitized Solar Cells (DSSC) I-V characterization process. The influence of the temperature and the light irradiance intensity on the I-V curves shape was given. Similarly, the impact of the voltage measuring scan speed, and direction were investigated. Furthermore, the effect of the cell shadowing mask, measuring probes positioning, and the averaging on the accuracy of performances measurement process were given.

Keywords—Dye Sensitized Solar Cells; I-V characteristics; temperature; measuring methods; sweep voltage scan; characteristic capacitance; active area

I. INTRODUCTION

Due to the fossil energy sources insufficient amount, renewable energy sources is the major solution to the rapidly increase in worldwide energy consumption. Photovoltaic solar cells are one of primary renewable energy source due to the important benefits [1]. Dye Sensitized Solar Cells (DSSCs) have the cleanest and lowest production cost and the easiest fabrication process regarding other Photovoltaic (PV) devices which make these cells very attractive and extremely promising [2-4]. Very recent confirmed tests show a 13% of efficiency under IEC 60904-3: 2008 and the American Society for Testing and Materials (ASTM) G-173-03 global standards [5]. Regarding the reported results, it is possible to consider the DSSCs for commercial use [6].

As several technics are used to evaluate “DSSCs” efficiencies [7-9], the accurate estimations, need for a unified and normalized method was essential. The “ASTM” advice is to use a stepwise varying bias voltage supply on the Device Under-Test (DUT) to obtain the current versus voltage (I-V) characteristic curves [10, 11]. Fig. 1 shows the power supply on a typical “DUT”.

This method has three important parameters: “ T_m ”, “ T_d ” and “ ΔV ”. Therefore, they must be suitable with the “DUT” morphology. The accuracy is the greatest advantage of this method. Voltage can rise in a range between a negative and a positive voltage. This offers the possibility to measure the full “I-V” cell characteristics. Moreover, sampling will be much accurate as the Source Measurement Unit (SMU) is excessively efficient.

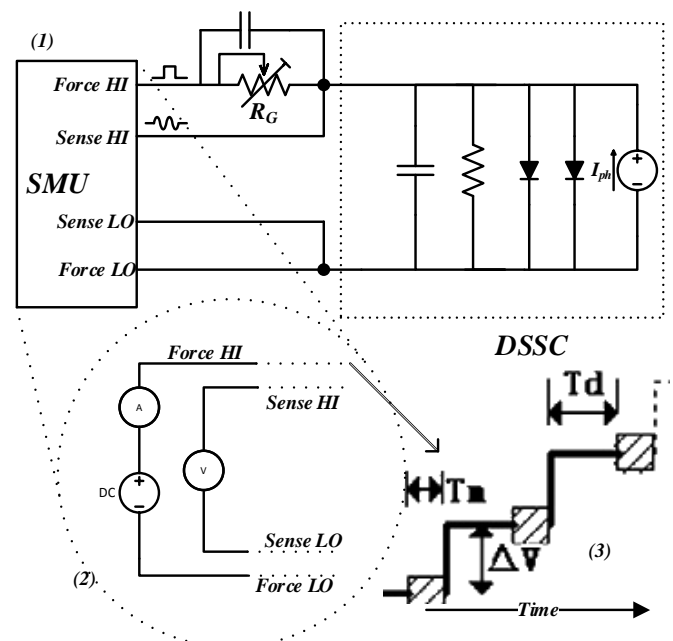


Figure 1: Measuring circuit configuration for a stepwise varying bias voltage supply on the “DUT”; (1) is the synoptic schematic; (2) present the measurement method configuration; (3) shows the stepwise signal, were “ T_d ” is the sampling time, “ T_m ” is the measuring time and “ ΔV ” is the stepwise voltage changing level [12].

II. EXPERIMENTAL MATERIALS

Along the tests, the lighting source was calibrated to simulate low intensity light levels: indoor lighting levels. Its maximum range is 40mW/cm^2 and based on a high intensity LEDs array. A double layer spectral correction filter and an electronic shutting system were used along the measurement. Fig. 3 presents the system irradiance spectrum. The measurement system use a lab developed Digital Acquisition Board (DAQ). It ensures to carry the experiments under a constant environment conditions with a high “I-V” measurement accuracy.

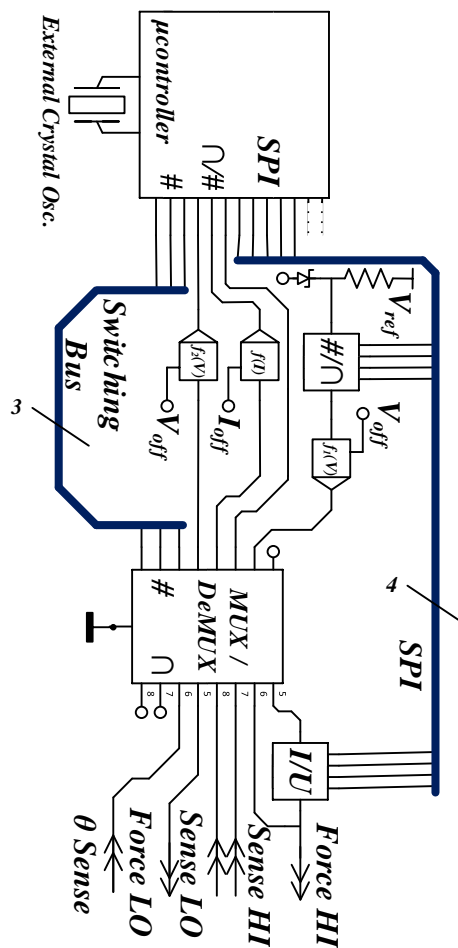


Figure 2: Experimental developed setup. Where θ Sense is the temperature sensing acquisition signal. The system uses the Serial Peripheral Interface (SPI) communication between different stages.

The measurement system was set to be suitable with DSSC measuring process. Thus, the “DAQ” is developed beneath a digitally controlled components with a supervision GUI (Graphic User Interface) allowing this system to reach a $200\mu\text{V}$ of voltage scan precision, $0.5\mu\text{A}$ of practical current measurement [13].

Also, a natural “DSSC” has been made for the experimental manipulation. In this work, the Doctor Blade technique was used to prepare the titanium dioxide nanoparticles film. The paste was made and arranged after extruding it onto a Fluorine doped Tin Oxide (FTO) glass surface. The prepared substrate has been heated on a hot plate [14].

The dye is extracted from the “*Hibiscus Sabdariffa*” plant leaves crashed in a juice mixer. After that, the powder (10 g) was soaked in a 250 ml Erlenmeyer flask with 80 ml of a pure ethanolic solution. The mixture was then filtered.

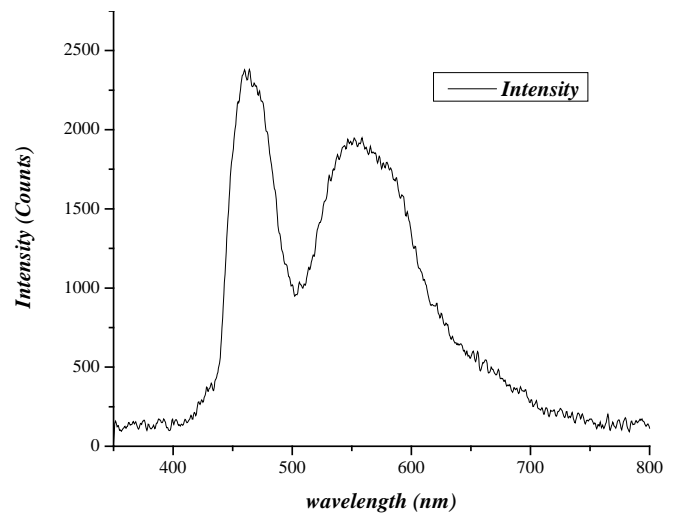


Figure 3: The lighting system irradiance spectrum



Figure 4: The Hibiscus Sabdariffa leaves

The TiO_2 substrate was dipping in the natural powder solution for the dye absorption after it was heat treated up to 450°C for a half of hour and then was allowed to cool down gradually. The cell photo-electrode has an area of 1.5 cm^2 . The counter-electrode was covered with a thin carbon layer deposited on the conductive face of the FTO glass using fumigation method. So, in cell assembly, the used electrolyte is a commercial volatile Triiodide solution.

III. RESULTS AND DISCUSSION

The Testbench of the DSSC is composed of the cell itself, the acquisition electronic system connected to a PC, a lighting source and a checker system equipped of an oscilloscope and a Keithley measurement unit to validate the measures if needed.

A. Lighting influence

1) Standard lighting conditions

Lighting is the most critical parameter in any Solar Cell (SC) characterization [15]. Thus, testing cells under a

standard lighting condition is obligatory for fair comparison between different researches group measurements. In the 1980s the US National Renewable Energy Laboratory (NERL), established the first “PV” characterization standards. The Standard Reporting Conditions (SRC) insist to measure cell performances with 1kW/m^2 of light irradiance and an (air mass) AM 1.5 of spectrum reference.

The irradiance in the characterization is usually measured using a reference “SC”. The presence of a mismatch between the spectral response of the reference detector and the “DUT”, or also, between the light source and the reference irradiance spectrum, produces an error in the “J-V” measurement. The measuring of light intensity is expressed by the short-circuit current “ I_{SC} ” of the reference device. Thus, the mismatch correction is shown as:

$$I_{SC} = \frac{I_{ref}^C \cdot I_{SC_m}}{M \cdot I_{ref}} \quad (1)$$

“ I_{ref} ” is the short circuit current of the reference cell and “ I_{ref}^C ” is its calibrated value under the lighting source. “ I_{SC} ” is the short circuit current under reference irradiance and “ I_{SC_m} ” is the measured short circuit current. “ M ” is the spectral mismatch correction factor [16]. This element is correlated with the spectral irradiance of the reference and the source, and the spectral responses of the “DUT” and the reference cell, including their ranges. Accurate results for international comparison are only the product of calibrated lighting sources. Therefore, they involve the knowledge of the spectral mismatch factor “ M ”. Therefore, the standards set the common measurement lighting condition to AM 1.5±25% of spectral distribution of the light and 1 sun ±2% of the measured irradiance at the surface of the solar cell [17].

2) Measures under various lighting intensity levels on DSSC performances

Light intensity affects the “PV” cells performances outcome from its influence on the cell parameters. However, it is important to examine the “SCs” under several environment conditions to understand the possible impacts.

Fig. 5 shows the “DSSC” equivalent circuit. Eq. (2) shows the static output of the cell, with which Eqs. (3) and (4) illustrate the open circuit voltage (V_{OC}) and the efficiency ratio “ η ” of the cell.

$$I = I_{ph} - I_0 \cdot \left(e^{\left(\frac{q \cdot (V - I \cdot R_s)}{K \cdot T \cdot n} \right)} - 1 \right) - \frac{V(t) + I \cdot \sum R_i}{R_{sh}} \quad (2)$$

Where “ I_0 ” and “ n ” are respectively the diode reverse current and ideality factor. “ K ” is Boltzmann’s constant and “ q ” is the elementary charge, “ I_{ph} ” is the photocurrent. All current derived parameters “ I_{SC} ”; “ I_{MAX} ” and the instantly delivered current “ I ” are in linearly relative with light intensity [18, 19].

$$V_{OC} = \frac{K \cdot T}{q} \ln \left(\frac{I_{ph}}{I_0} + 1 \right) \quad (3)$$

$$\eta(\%) = \frac{P_{max}}{E_{tot} \cdot A} \cdot 100 \quad (4)$$

“ E_{tot} ” is the total incident light power measured in Watt per meter square (W/m^2), and “ A ” is the cell active area.

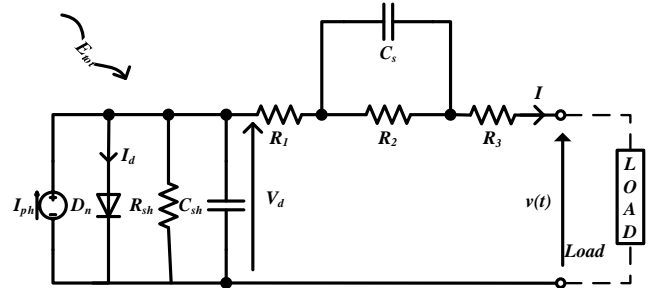


Figure 5: “DSSC” equivalent circuit (single diode model) [13, 20]

Fig. 6 shows the “DSSC” “J-V” measurement under several irradiance intensity levels of the light source. Measures are taking beneath ambient temperature.

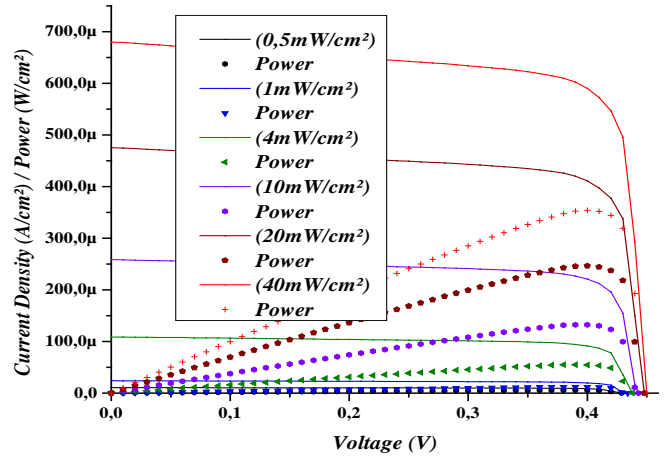


Figure 6: “DSSC J-V” curves under several irradiance levels.

Curves show that power, as the “DSSC I_{SC} ”, increases with lighting level elevation. Nonetheless, the cell efficiency increases until a border value as showing in Fig. 8. Likewise, the “ V_{OC} ” values presented in Fig. 7 will reach their limit sooner than “ I_{SC} ” ones. These demonstrate that the dependence of “ V_{OC} ” by the lighting intensity may explain the boundary value of the efficiency presented on Fig. 8. Undeniably, the “DSSC V_{OC} ” values are in logarithmic dependency with light intensity.

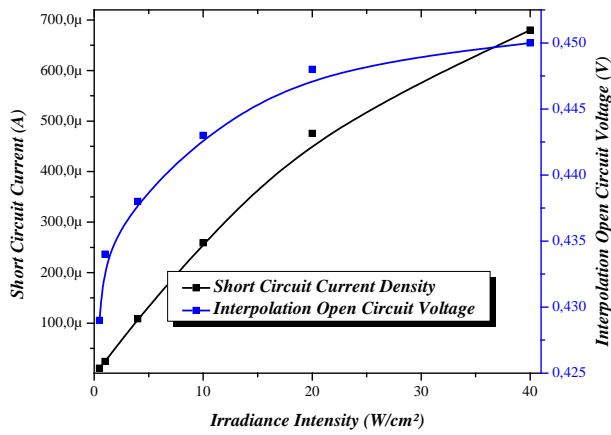


Figure 7: Dependence of “ V_{OC} ” with varying irradiance intensity.

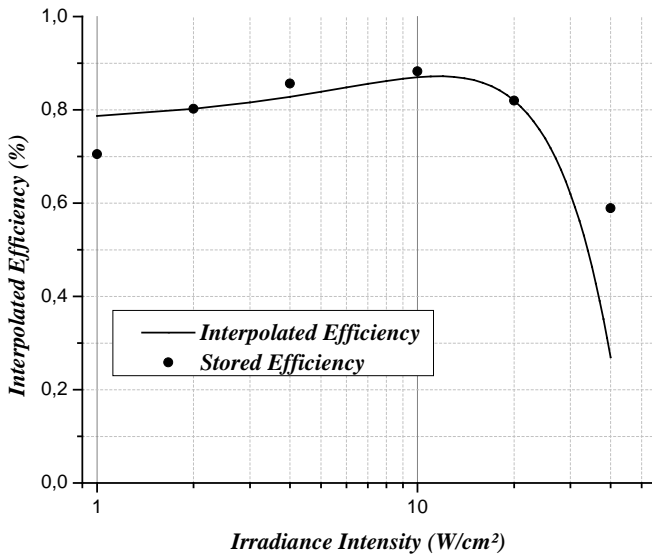


Figure 8: Dependence of “ η ” with irradiance intensity.

Staring the Fig. 8, the “DUT” has 0.88% of maximum efficiency and it has reached at 10mW/cm². This value of irradiance intensity is far from the standard used lighting level (100mW/cm²). This concluding that concentrating system can augment cell output power, nonetheless it will affect the dye cell efficiency unlike Silicon “Si” cells [21].

3) “DSSC” Active area

The area of “PV” cell is its frontal area including grids and contact [22]. Thus, for accurate “J-V” measurement, it is critical to ensure that “DSSC” defined area is only the active region space. Shadowing masks are used to determinate the active cell area. The space of the aperture mask prevents any outside light collection by the cell. This technic prevents artificial growth of measured values and the minimum active area for standard efficiency measuring is 1cm². Correct “DSSC” active area measurement increases the accuracy of the performances measurement as shown in Eq. (4). “DSSCs” do not have a smooth edged electrode. Therefore, it is difficult to accurately determinate the cell active area.

Regarding more accuracy, it is preferred to use microscope to measure it, and drill a shading mask to limit the extra-lighting on the cell surface. The evaporation of volatile solution in the composition of “DSSCs” generates significant errors in performances measurement. Beside the shading mask, it is important to control the thin layers status before setting the active area. A good encapsulation for the cell and using a cooling system to control its temperature can minimize the thin layers evaporation.

B. Temperature influence on “DSSC” performances

Temperature has an important influence on “DSSCs” performances. That is because the heat changes the physical proprieties of the device. The Standard Testing Conditions (STC), given by the “ASTM” standards, requires that measurement must be doing under $25\pm 1^\circ\text{C}$. “J-V” characterization can be a subject to a number of errors. “STC” arise some correctable ones since the respect of intruded test conditions. The correction of the measured current “ I_m ” is given in Eq. (5), were “ $\alpha_{I_{SC}}$ ” is the temperature coefficient for “ I_{SC} ” and “ T_0 ” is the nominal temperature value (25°C). When using a “SMU”, only current values are in correction. Voltage errors are eliminated as it is already imposed by the source.

$$I = I_m \frac{1}{1 - \alpha_{I_{SC}} (T_{DSSC} - T_0)} \quad (5)$$

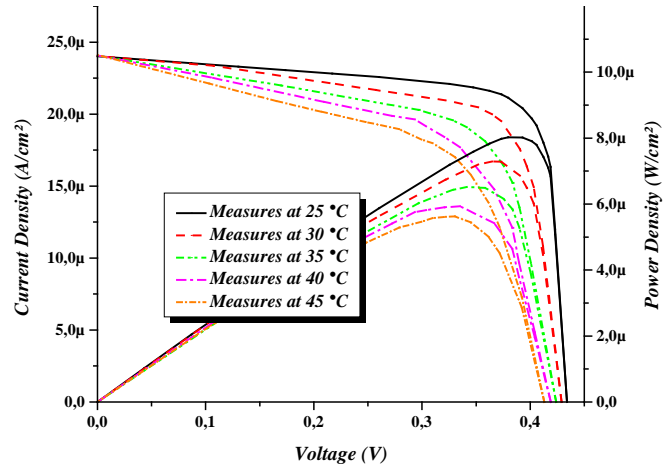


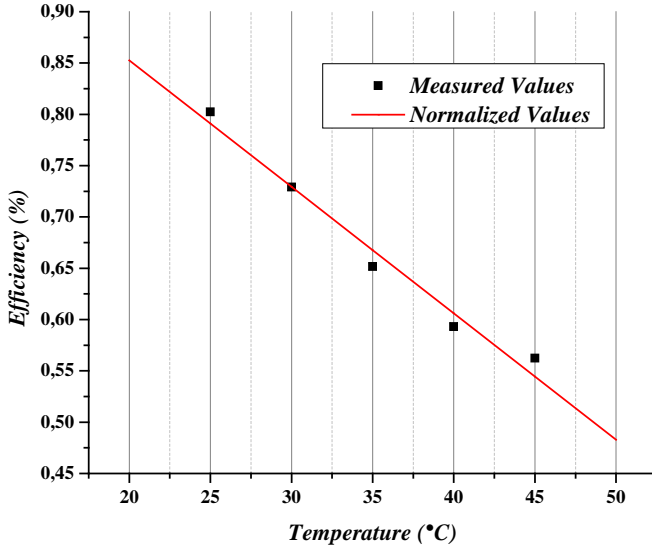
Figure 9: Influence of temperature on “J-V” curves shape

The Fig. 9 presents the “DSSC J-V” measurements under 20°C of temperature variation for the nominal value. As shown, temperature slightly affects the cell current density “ J_{SC} ” by increasing it in order of 1%. Nonetheless, “ V_{OC} ” is considerably sensitive regarding it [23]. The Fig. 10 represents the temperature dependence of the cell performances and parameters [24]. As showing, “ V_{OC} ” has decreased linearly by $\sim 5\%$. The rate of decline is $\sim 1.1\text{mV}/^\circ\text{C}$. Likewise, the characteristic resistances of the cell decreases, that affect the cell output power. Moreover, even if current density increased with $\sim 1\%$ with temperature, the overall performance of the cell has decreased by $\sim 1.2\%$.

Table 1: Variation of I-V parameters under various temperature values of the DSSC.

Temperature [°C]	V_{OC} [mV]	J_{SC} [$\mu\text{A}/\text{cm}^2$]	P_{max} [W/cm^2]
25	433,7	23,98	8,023
30	428,9	24,07	7,288
35	424,0	24,20	6,515
40	419,3	24,24	5,933
45	413,0	24,33	5,623

Sensing and controlling temperature of the “DUT” is highly recommended for accurate cell characterization. The measurement uncertainty depends on the measurement operation scenario. The most accurate process is when the system presents a temperature sensor with direct control option. Uncertainty is higher when the measurement scenario does not present a temperature sensor or a control option. The inexistence of the both of them makes uncertainty at highest value.


Figure 10: Dependence of cell efficiency with varying temperature.

Conversely, as the “DSSC” has transparent glass, or plastic, package, the illumination during the measurement perturb the cell temperature from the nominal value. Ideally, measures must be taking at 25°C of temperature. Unlike conventional “Si” solar cells, where it is possible to avoid temperature perturbation by soaking the cell under illumination until the equilibration of the temperature, “DSSC” under tests present a problem of evaporation of the thin films of the cell, which decrease the cell performance intensely [25]. In case of sol-gel based “DSSC”, the temperature equilibrium can be reached by the same method as “Si” cells [26]. This eliminates the application of the temperature coefficient “ $\alpha_{I_{sc}}$ ” in the current correction. As well, the expression of the current measurement correction, as presented in Eq. (1) & (5), is accomplished by the Eq. (6).

$$I = I_m \cdot \left(\frac{I_{ref}^c}{I_{ref}} \right) \cdot \left(\frac{1}{M} \right) \cdot \left(\frac{1}{1 - \alpha_{I_{sc}} (T_{DSSC} - T_0)} \right) \quad (6)$$

Temperature can be measured with “RTD” (Resistance Temperature Detectors) or thermocouple sensors. The measuring device carcass must be set in direct contact with the cell back electrode. A reference “DSSC” cell has a temperature-sensing device built into the cell package for more accurate heating measurement.

C. Voltage bias scan speed calibration

The accurate method for determining “DSSC” efficiency is measuring its output power, using “J-V” characteristics, when a stepwise change of voltage supply cross the cell (Fig. 1). Voltage supply sampling time (T_d) must be four times further than the time constant of the “PV” cell (τ) [10]. Regarding the high capacitance value of “DSSCs”, “ T_d ” must be a number of seconds to achieve transient photocurrent equilibrium after changing the stepwise voltage. Although, using long delays with elevated number of measurement points, to afford more accuracy, provide temperature increasing. More heating can damage the cell and degrade its efficiency as showing before [27]. Scan speed must be fast to evade the irradiation beam effect on the cell. Nonetheless, reaching accuracy with this method is not so trivial. In Fig. 5, we can determine the equation of the dynamic output characteristics curves of the “DSSC” regarding its capacity as shown by this equation:

$$I = I_{ph} - I_0 \cdot \left(e^{\left(\frac{q}{K.T.n} (V(t) + I.R_s) \right)} - 1 \right) - \frac{(V(t) + I.R_s)}{R_{sh}} \quad (7)$$

$$+ (C_s + C_{sh}) \cdot R_s \cdot \frac{dI(t)}{dt} + C_{sh} \cdot \frac{dV(t)}{dt}$$

For this evaluation, the series resistances are neglected [28]. Accordingly, the output characteristic can be expressed as follow:

$$I = I_{ph} - \frac{V_d}{R_{sh}} + C_{sh} \cdot \frac{dV}{dt} \quad (8)$$

Hence, the influence of the capacitance in the current expression is relative to the term dV/dt , which is the expression of the scan speed. Thus, an excessive scan speed will distort the “J-V” curves as is showing in Fig. 11. Furthermore, to limit this defect, the capacitance delay must be measured using the charging and discharging effect on the cell output. The accuracy is highest when the choice is based on a compromise between the number of measurement points and the scan delay, which can provide a fast scan without heating the cell.

As a final point, sampling delay “ T_d ” must be suitable with the number of the measuring points to avoid cell heating. To reach a high accuracy with fast measurement, scan speed must be regulating to recompense the choosing value of “ T_d ”, and lessens the influence of the capacitance in the scan. Every DSSC have its appropriate scanning speed, therefore, its value must be calculated with the estimated cell capacitance. These estimations are useful to measure “DSSCs” efficiency more accurately and rapidly.

D. Scanning directions

The irradiance beam perturbs the cell temperature as showing before. Therefore, in case of cell heating, the voltage scan should be in reverse, beginning from the “ V_{OC} ”, which is very sensitive to temperature than the “ I_{SC} ”, to 0V rather the other direction (direct scan). In other hand, the characteristic capacitance has a huge pretend on the scan direction as shown in the figure below.

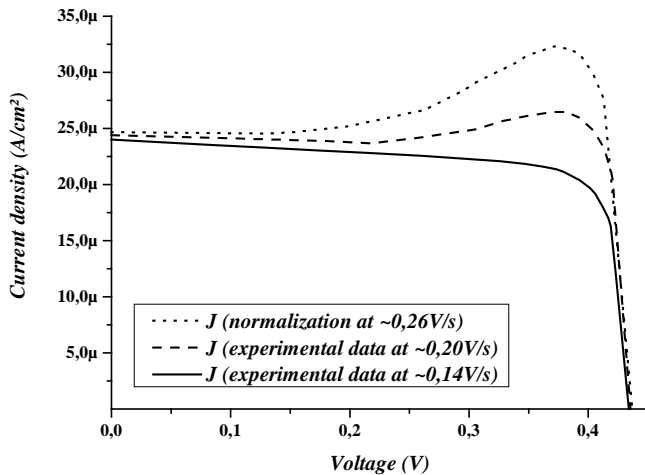


Figure 11: Influence of cell capacitance on “J-V” curves.

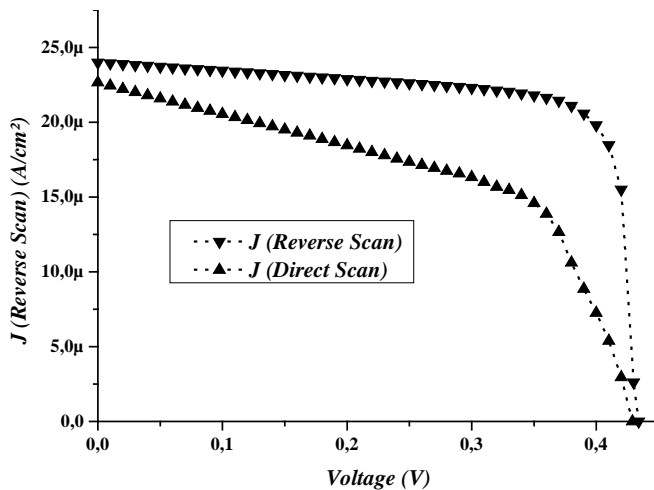


Figure 12: Dependence of “J-V” curves with scanning direction

A noticeable difference between the reverse and normal sweep is observed in the DSSC J-V characteristics. The figure shows clearly that all the cell performances increase in reverse scan (V_{OC} , J_{SC} , η and FF). This phenomenon depends on the cell capacitance, hence the scan speed. Decreasing voltage bias speed minimizes the difference between the two scan-directions. It is required to use the average values of the obtained measurement from the both scan directions. Previous researches proved that “DSSC” average performances does not depend on the cell scan direction. In addition, the new average values reflects the exact “J-V” characteristics [8]. In addition, it is extremely required to execute several back and forth voltage sweep scans before

implementing the averaging. The figure below shows the effect of averaging with various scan repetition.

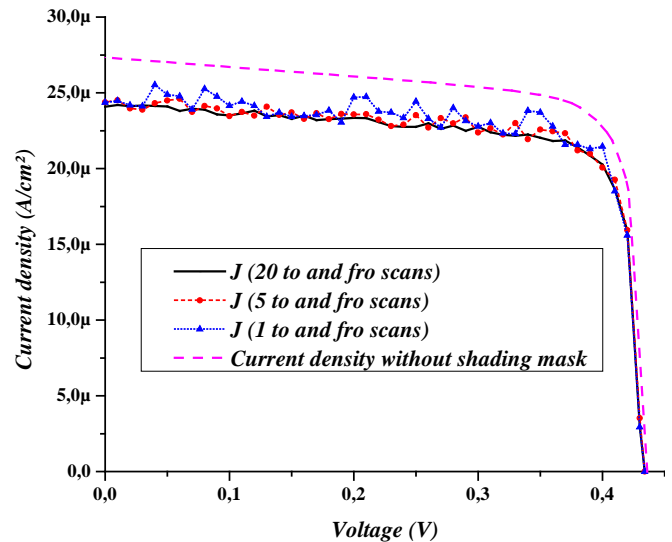


Figure 13: Averaging effect on “J-V” curves

E. Acquisition probes

Precise systems use a Kelvin clip to acquire “DSSC” electrical performance. Four terminals (4T), as “Force” and “Sense”, reassure a high accurate current and voltage measuring. The use of these terminals eliminates the lead and the contact resistance, which can destruct the characteristics curve shape. This technic consists to source the voltage over one lead (Force HI) and sense it with the two others (Sense HI and Sense LO) attached to the cell terminals (A^- and K^+). This might ensure the real value of the developed voltage exciting the cell. “Force HI” probe contains an accurate low current sensor to measure “J-V” characteristics. To avoid noise, probes must be attached to coaxial cables with common ground connection. In addition, probes can be covered with matt gum to avoid light reflection, which affect the “STC” of the cell test [27, 29].

IV. CONCLUSION

In this paper, we have studied the Dye Sensitized Solar Cells “I-V” characterization process. Both temperature influence and irradiation intensity impact on the cell measurement has been discussed and analyzed with details. Likewise, the scan speed, directions and process has been discussed in order to obtain an accurate characterization process for the “DSSC”.

REFERENCES

- [1] Lafi Al-Otaibi, “Intelligent Energy Management in a Photovoltaic Installation Using Fuzzy Logic”, *International Journal of Science and Techniques of Automatic control & computer engineering IJ-STA*, vol. 5, no. 2, pp. 1567-1585, December 2011.
- [2] Simon Mathew, "Dye-sensitized solar cells with 13% efficiency achieved through the molecular engineering of porphyrin sensitizers", *Nature Chemistry*, vol. 6, pp. 242–247, 2014.

- [3] Ran Miao et Al., "Mesoporous TiO₂ modified with carbon quantum dots as a high-performance visible light photocatalyst", *Applied Catalysis B: Environmental*, vol. 189 no. 4, pp 26-38, February, 2016.
- [4] Stephen Lourens Tanihaha, "Fabrication and Characterization of Dye-sensitized Solar Cell using Blackberry Dye and Titanium Dioxide Nanocrystals", in *Second International Conference on Advances in Computing, Control, and Telecommunication Technologies*, Jakarta, 2010.
- [5] Martin A. Green et Al., "Solar cell efficiency tables (Version 46)", *Progress in Photovoltaics: Research and Applications*, vol. 23, pp 805–812, May, 2015.
- [6] Paramaguru Ganesan, "Unravel the Impact of Anchoring Groups on the Photovoltaic Performances of Diketopyrrolopyrrole Sensitizers for Dye-Sensitized Solar Cells", *ACS Sustainable Chemistry & Engineering*, Aug., 2015.
- [7] F. Granek, "Advanced System For Calibration And Characterization Of Solar Cells", *Opto-Electronics Review*, vol. 12, no. 1, pp. 57–67, 2004.
- [8] Naoki Koide, "Measuring methods of cell performance of dye-sensitized solar cells", *Rev. Sci. Instrum.*, vol. 75, no. 2828, 2004.
- [9] JA. Ramos-Hernanz, "Obtaining the characteristics curves of a photocell by different methods", in *International Conference on Renewable Energies and Power Quality*, Bilbao, 2013
- [10] Hanmin Tian, "Influence of capacitance characteristic on I–V measurement of dye-sensitized solar cells", *Measurement*, vol. 44, no. 9, Pages 1551–1555, November, 2011.
- [11] L. Bouslimi et Al., "Electric and spectral characterization of a high pressure mercury lamp used in the photochemical treatment", *International Journal of Science and Techniques of Automatic control & computer engineering IJ-STA*, vol. 3, no. 2, pp 1064-1071, December 2009.
- [12] A. Maoucha, F. Djeflal et Al., "An accurate Organic solar cell parameters extraction approach based on the illuminated I–V characteristics for double diode modeling", in *First International Conference on Renewable Energies and Vehicular Technology*, Hammamet, 2012.
- [13] A. E. Touihri et Al., "Specific digital characterization system for dye sensitized solar cells", in *International Conference on Electrical Sciences and Technologies in Maghreb (CISTEM)*, Tunis, 2014
- [14] A. Torchani et Al. "Sensitized solar cells based on natural dyes", *Current Applied Physics*, vol. 15, no. 3, pp 307-312, March, 2015.
- [15] V. Shrotriya, "Accurate Measurement and Characterization of Organic Solar Cells", *Advanced Functional Materials*, vol. 16, no. 15, pp. 2016–2023, October, 2006.
- [16] J. M. Kroon, "Accurate efficiency determination and stability studies of conjugated polymer/fullerene solar cells. *Thin Solid Films*, vol. 404-405, pp.223-228, 2002.
- [17] *Extraterrestrial Spectrum, Terrestrial Global 37 deg South Facing Tilt & Direct Normal + Circumsolar*, ASTM G-173-03, 1992
- [18] A. El-Shaer, "Effect of Light intensity and Temperature on Crystalline Silicon Solar Modules Parameters", *International Journal of Emerging Technology and Advanced Engineering*, vol. 4, no. 8, August, 2014
- [19] Badii Bouzidi et Al., "The Classical and Analytic DTC for Photovoltaic Panel Position and Control", *International Journal of Science and Techniques of Automatic control & computer engineering IJ-STA, Special Issue, CEM*, pp. 636-651, December 2008.
- [20] T. Azizi, A.E. Touihri et Al., "Comparative study between dye-synthesized solar cells prepared by electrophoretic and doctor blade techniques", *Optik - International Journal for Light and Electron Optics*, vol. 127, no. 10, Pages 4400–4404, May, 2016.
- [21] Liyuan Han, "Modeling of an equivalent circuit for dye-sensitized solar cells: improvement of efficiency of dye-sensitized solar cells by reducing internal resistance", *Comptes Rendus Chimie*, vol. 9, no. 5–6, pp. 645–651 May–June, 2006
- [22] *Standard Test Method for Electrical Performance of Non-Concentrator Photovoltaic Cells Using Ref. Cells*, ASTM E948, 2015
- [23] Akira Usami, "Temperature dependence of open-circuit voltage in dye-sensitized solar cells", *Solar Energy Materials and Solar Cells*, vol. 93, no. 6–7, pp.840–842, June, 2009
- [24] Priyanka Singh, "Temperature dependence of I–V characteristics and performance parameters of silicon solar cell", *Solar Energy Materials and Solar Cells*, vol. 92, no. 12, pp. 1611-1616, Dec., 2008
- [25] F. Anderson S. Lima, "Electrochemically synthesized mesoporous thin films of ZnO for highly efficient dye sensitized solar cells", *Ceramics International*, vol. 41, no. 8, pp. 9314–9320, September 2015
- [26] Kirti Sahu, "Novel sol gel method of synthesis of pure and Aluminum doped TiO₂ nano particles useful for dye sensitized solar cell applications", *International Research Journal of Engineering and Technology*, vol. 02, no. 04, July, 2015
- [27] *Procedures for temperature and irradiance corrections to measured I-V characteristics*, IEC 60891, 2009
- [28] K. Bouzidi, "Solar cells parameters evaluation considering the series and shunt resistance", *Solar Energy Materials & Solar Cells*, vol. 91, pp. 1647–1651, 2007
- [29] *Standard Procedures for Terrestrial Photovoltaic Measurements*, EUR-7078 EN, 1979